Analyzing Multi-Fiber Reconstruction in High Angular Resolution Diffusion Imaging using the Tensor Distribution Function

Liang Zhan[1], Alex D.Leow[1,2], Siwei Zhu[3], Ming-Chang Chiang[1], Marina Barysheva[1], Arthur W. Toga[1], Katie L. McMahon[4], Greig I. de Zubicaray[4], Margaret J. Wright[5], Paul M. Thompson[1]

[1]Laboratory of Neuro Imaging, Department of Neurology, UCLA School of Medicine, UCLA, Los Angeles, CA

[2]Neuropsychiatric Institute, UCLA School of Medicine, Los Angeles, CA

[3]Department of Mathematics, UCLA, Los Angeles, CA

[4] University of Queensland, Functional MRI Laboratory, Centre for Magnetic Resonance, Brisbane, Australia

[5]Queensland Institute of Medical Research, Brisbane, Australia

ABSTRACT

High-angular resolution diffusion imaging (HARDI) can reconstruct fiber pathways in the brain with extraordinary detail, identifying anatomical features and connections not seen with conventional MRI. HARDI overcomes several limitations of standard diffusion tensor imaging, which fails to model diffusion correctly in regions where fibers cross or mix. As HARDI can accurately resolve sharp signal peaks in angular space where fibers cross, we studied how many gradients are required in practice to compute accurate orientation density functions, to better understand the trade-off between longer scanning times and more angular precision. We computed orientation density functions analytically from tensor distribution functions (TDFs) which model the HARDI signal at each point as a unit-mass probability density on the 6D manifold of symmetric positive definite tensors. In simulated two-fiber systems with varying Rician noise, we assessed how many diffusion-sensitized gradients were sufficient to (1) accurately resolve the diffusion profile, and (2) measure the exponential isotropy (EI), a TDF-derived measure of fiber integrity that exploits the full multidirectional HARDI signal. At lower SNR, the reconstruction accuracy, measured using the Kullback-Leibler divergence, rapidly increased with additional gradients, and EI estimation accuracy plateaued at around 70 gradients.

Index Terms— High Angular Resolution Diffusion Imaging, Tensor Distribution Function, multi-fiber construction, Kullback-Leibler divergence, Exponential Isotropy

1. INTRODUCTION

Diffusion weighted MR imaging is a powerful tool to study water diffusion in tissue, providing vital information on white matter microstructure, such as fiber connectivity and composition in the healthy and diseased brain. To date, most diffusion imaging studies (especially in clinical applications) still employ the *diffusion tensor imaging* (DTI) model [1], which describes the anisotropy of water diffusion in tissues by estimating, from a set of *K* diffusion-sensitized images, the 3x3 *diffusion tensor* (the covariance matrix of a 3-dimensional Gaussian distribution). Each voxel's signal intensity in the *k*-th image is attenuated, by water diffusion, according to the Stejskal-Tanner equation [2]: $S_k = S_0 \, exp\,[-b g_k^T D g_k]$, where S_0 is the non-diffusion weighted signal intensity, D is the 3x3 diffusion tensor, g_k is the direction of the diffusion gradient and *b* is Le Bihan's factor containing information on the pulse sequence, gradient strength, and physical constants. Although 7 gradients are mathematically sufficient to determine the diffusion tensor, MRI protocols with higher angular and radial resolutions, such as the high-angular resolution diffusion imaging (HARDI) technique, can resolve more complex diffusion geometries that a single-tensor model, as employed in standard DTI, fails to capture, e.g. fiber crossings and intermixing of tracts.

Recent technical advances have made HARDI more practical. A 14-minute scan can typically sample over 100 angles (with 2 mm voxels at 4 Tesla). HARDI's improved signal-to-noise ratio can be used to reconstruct fiber pathways in the brain with extraordinary angular detail, identifying anatomical features, connections and disease biomarkers not seen with conventional MRI. If more angular detail is available, fiber orientation distribution functions (ODFs) may be reconstructed from the raw HARDI signal using Q-ball imaging technique [3]. Deconvolution methods [4,5] have also been applied to HARDI signals, yield mathematically rich models of fiber geometries as probabilistic mixtures of tensors [6], fields of von Mises-Fisher mixtures [7], or higher-order tensors (i.e., 3x3x…x3 tensors) [8,9]. Stochastic tractography [10, 11] can also exploit HARDI's increased angular detail, and fluid registration methods have also been developed to align HARDI ODFs using specialized Riemannian metrics [12]. In most deconvolution-based methods, however, restrictive prior assumptions are typically imposed on the allowable fibers, e.g., all fiber tracts are considered to have the same anisotropy profile.

A novel approach, the Tensor Distribution Function (TDF), was recently proposed by Leow et al. in [13] to model multidirectional diffusion at each point as a probabilistic mixture of all symmetric positive definite tensors. The TDF models the HARDI signal more flexibly, as a unit-mass probability density on the 6D manifold of symmetric positive definite tensors, yielding a TDF, or continuous mixture of tensors, at each point in the brain.

From the TDF, one can derive analytic formulae for the orientation distribution function (ODF), tensor orientation density (TOD), and their corresponding anisotropy measures. Because this model can accurately resolve sharp signal peaks in angular space where fibers cross, we studied how many gradients are required in practice to compute accurate orientation density functions - as more gradients require longer scanning times. In simulated two-fiber systems with varying Rician noise, we assessed how many diffusion-sensitized gradients were sufficient for (1) accurately resolving the diffusion profile, and (2) measuring the exponential isotropy (EI), a TDF-derived measure of fiber integrity that exploits the full multidirectional HARDI signal.

2. METHOD

We created various models of two-fiber systems, crossing at 90 degrees with equal volume fractions (w_1=w_2=0.5). Here we chose λ_1=10x10^{-10} m^{2}s^{-1} and λ_2=2x10^{-10} m^{2}s^{-1} as the eigenvalues for each individual tensor (FA=0.77, typical for white matter) and we added Rician noise with different amplitudes (SNR=5, 15, 25) (with a standard deviation of S(0)/SNR) to generate simulations using discrete mixtures of Gaussian distributions:

$$\frac{S(q)}{S(0)} = \sum_{i=1}^{2} w_i \exp(-tq^T D_i q) + noise \qquad (1)$$

Data were sampled at 94 points evenly distributed on the hemisphere whose distribution was computed using a Partial Differential Equation (PDE) based on electrostatic repulsion [14]; we chose 94 as it is the same as the number of gradients in a large ongoing HARDI study [13]. Several angular sampling schemes, with between 6 to 94 directions, were sub-sampled from the original 94 angular points to maximize the total angular energy. The angular distribution energy between point *i* and point *j* is denoted as E_{ij}, which is defined as the sum of the squares of the least spherical distance between point *i* and point *j* and the least spherical distance between point *i* and point *j*'s antipodal symmetrical point *J*:

$$\mathrm{E_{ij}} = \mathrm{dist^2(i,j)} + \mathrm{dist^2(i,J)} \qquad (2)$$

Here, *i,j* are two different points in the spherical surface, *J* is the antipodally symmetric point of *j*, and dist(i,j) is the least spherical distance between point *i* and point *j*. The total angular distribution energy for one gradient subset with *N* diffusion-sensitized gradients was defined as the summation of angular distribution energy between all pairs points, using geodesic distances on the sphere:

$$\mathrm{E(N)} = \sum_{\mathrm{i=1}}^{\mathrm{N}} \sum_{\mathrm{j=1}}^{\mathrm{N}} \mathrm{E_{ij}} \quad (\mathrm{i} \neq \mathrm{j}) \qquad (3)$$

We first chose one seed point from the original 94 points, which (without loss of generality) was (1,0,0) in our study, then found another 5 points from the remaining 93 points to maximize E(6) since 6 diffusion sensitized gradients are the minimum required for tensor estimation. So the first subset with 6 diffusion sensitized gradients was produced. After this basic subset, we artificially increased the angular sampling one by one by maximizing E(7), E(8),…E(93). E(94) represents the sample of our original HARDI data.

Using these optimized subsets of angular points, we sub-sampled the original HARDI94 data, and the TDF method was used to analyze the subsampled images. We denote the space of symmetric positive definite three-by-three matrices by $\mathbb{D}$. The probabilistic ensemble of tensors, as represented by a tensor distribution function (TDF) *P*, is defined on the tensor space $\mathbb{D}$ that best explains the observed diffusion-weighted images:

$$S_{calculated}(q) = \int_{D\in\mathbb{D}} P(D) \exp(-tq^t Dq)\, dD \qquad (4)$$

To solve for an optimal TDF *P**, we use the multiple diffusion-sensitized gradient directions q_i and arrive at *P** using the least-squares principle:

$$P^* = argmin_p \sum_i \left(S_{obs}(q_i) - S_{calculated}(q_i)\right)^2 \qquad (5)$$

From the TDF, the orientation density function (ODF) can be analytically computed from Eq. 6:

$$ODF(\tilde{x}) = C \int_{D\in\mathbb{D}} P(D)(\det(D)\, \tilde{x}^t D^{-1} \tilde{x})^{-\frac{1}{2}} dD \qquad (6)$$

These ODFs were rendered using 642 points, determined using a seventh-order icosahedral approximation of the unit sphere.

To assess how accurately the diffusion profiles could be reconstructed in situations based on different angular sampling schemes, the Kullback-Leibler (KL) divergence, a commonly used measure from information theory, was used to measure the discrepancy, between the reconstructed and ground truth ODFs. Reconstruction error was calculated from Eq.7, in which *p(x)* is the ODF derived from the subsampled schemes with additive Rician noise of various amplitudes, while *q(x)* is the noise-free ODF derived from the ground truth data.

$$sKL(p,q) = \frac{1}{2}\int_{\Omega} \left\{p(x)\log\left(\frac{p(x)}{q(x)}\right) + q(x)\log\left(\frac{q(x)}{p(x)}\right)\right\} dx \qquad (7)$$

Lastly, we also computed another measure proposed in the original TDF framework, the *exponential isotropy* (EI; Equation 8). Given any TDF *P*, the exponential isotropy quantifies the overall isotropy of any given voxel, and highlights the gray matter instead of white matter as in FA (since gray matter voxels tend to have low anisotropy, or high isotropy, and thus high EI values; see **Figure 1**)

$$EI\big(P(D)\big) = e^{-\int_{D\in D} P(D)\log P(D) dD} \qquad (8)$$

3. RESULTS AND DISCUSSION

Figure 2 shows several characteristic ways in which the additive Rician noise was seen to affect the reconstructed ODFs. The noise effects on HARDI ODF included combinations of local diffusion coefficient swelling, incorrect rotations of the dominant fiber directions, as well as mixing or omission of peaks in the radial fiber profile.

Figure 3 shows how the angular resolution of the diffusion gradient set affects the HARDI ODF. The higher the angular resolution, the more accuracy ODF can be

recovered; even so, reconstruction errors vary from angular smearing and coalescing of the ODF peaks between 40 and 60 gradients [(e)-(g)] to incorrect recovery of the dominant fiber direction at 30 gradients (d), which could be problematic for ODF-based tractography.

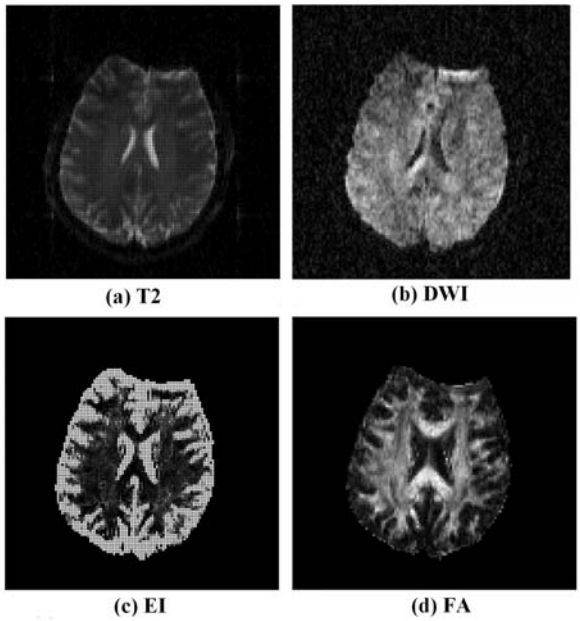

Figure 1. Comparing EI with FA.
This figure shows (a) T2-weighted image (b) DWI image (c) EI plot and (d) FA plot. These figures are computed from 94-direction human brain HARDI data (4 Tesla; *b*-value: 1159sec/mm^2; TE/TR: 92.3/8250 msec; FOV=230x230; in-plane resolution: 1.8x1.8mm; 55x2mm^2 contiguous slices; acquisition time: 14.5 min). Comparing (c) and (d), we note that EI highlights the gray matter while FA emphasize the white matter. This is because gray matter voxels tend to have low anisotropy, or high isotropy, and thus high EI values. EI is an analog of the standard FA derived from the full HARDI gradient set; FA can be problematic as it poorly reflects (typically underestimates) the anisotropy of the component fibers when fibers mix or cross within a voxel; EI however, uses the full tensor distribution function to weight the estimated anisotropy.

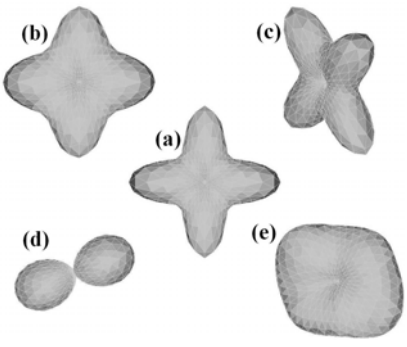

Figure 2. Noise effects on the HARDI ODF.
These glyphs show characteristic types of reconstruction errors that resulted from adding Rician noise to a simulated 2-fiber system, and deriving an ODF from the tensor distribution function. (a) Ground truth ODF; (b) swelling of the local diffusion coefficient; (c) incorrect rotations of the dominant fiber directions (this is a rotation out of the plane of the page); (d) omission of a dominant direction; (e) mixing of the dominant directions. All these ODF are calculated based on Equation 5 in the TDF framework without any regularization. Overall, the effect of noise on the HARDI ODF will most likely induce combinations of each of these types of distortion.

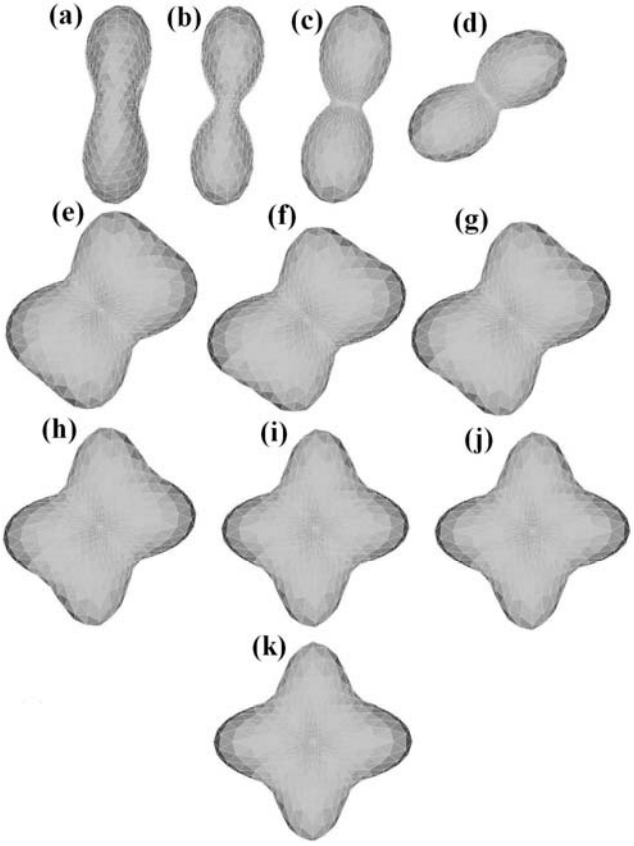

Figure 3. Angular resolution effects on the HARDI ODF
This figure illustrates how angular resolution affects HARDI ODF, which was calculated in the TDF framework based on Equation 5, without any regularization. ODFs are reconstructed from sets of progressively more gradients, in directions that optimize the angular distribution energy (Eq. 3): (a) HARDI-6 (b) HARDI-10 (c) HARDI-20 (d) HARDI-30 (e) HARDI-40 (f) HARDI-50 (g)HARDI-60 (h) HARDI-70 (i) HARDI-80 (j) HARDI-90 (k) HARDI-94.

To quantify the accuracy of ODF recovery at different SNR levels and at different angular resolutions, the reconstruction error, represented by the sKL divergence, was calculated. As expected, sKL decreased with increasing SNR and when using more scanning directions (**Figure 4**). The reconstruction accuracy of a 90-direction low-SNR sequence was about the same as a 7-direction sequence with five times the SNR. Our simulation studies show that when SNR is low, adding directions has greater benefit.

EI, a measure of fiber integrity related to FA (but avoiding the limitations of the single-tensor model), decreases with increasing angular resolution, stabilizing by ~70 directions (Figure 5). This is in line with the finding

that fractional anisotropy, derived from DTI, is generally underestimated when fibers cross. Also, this result is consistent with **Figure 3,** which shows that HARDI70 has satisfying results when reconstructing a two-fiber crossing at 90 degree; these diagrams make it clearer why the isotropy falls (i.e., anisotropy rises) when the two peaks no longer coalesce.

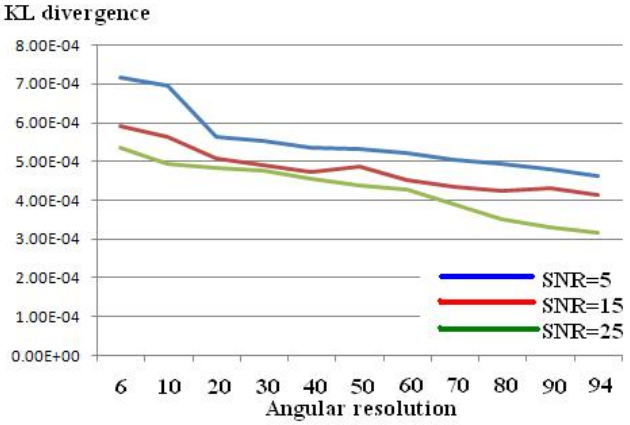

Figure 4. KL-divergence (reconstruction error) vs. Angular resolution

For each angular resolution scheme, 1000 simulations of two-tensor systems (equal volume fractions; 90º crossing) were computed with different SNR. This figure shows that the sKL divergence (reconstruction error) decreases with the increasing SNR level, as well as when using higher angular sampling schemes. This means that the accuracy of the computed ODF improves as SNR increases and angular resolution increases.

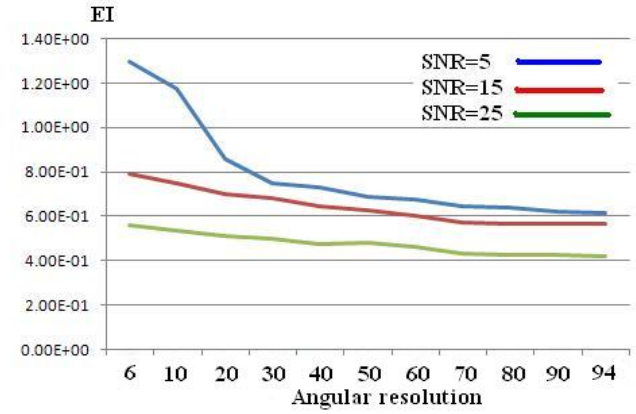

Figure 5. Estimates of Exponential isotropy (EI) vs. Angular resolution

For each angular resolution scheme, 1000 simulations of two-tensor systems (equal volume fractions; 90^0 crossing) were computed with different SNRs. The EI decreases with the increasing SNR level, as well as using higher angular sampling schemes. Also, EI tends to stabilize when the angular resolution reaches ~70 gradients. This is in line with the observation that standard FA measures are biased (too low) in regions where fibers mix or cross.

4. CONCLUSION

HARDI scanning allows better diffusion reconstruction than DTI, at the expense of longer scanning times. We identified several types of ODF reconstruction error and studied their asymptotics in optimized angular sets. To improve diffusion reconstruction accuracy and remove bias from the derived anisotropy measures, it is more effective to acquire additional angular samples rather than to repeatedly sample the same directions for purposes of signal averaging.

5. REFERENCES

1. Basser PJ, Pierpaoli C. Microstructural and physiological features of tissues elucidated by quantitative diffusion tensor MRI. J. Magn. Reson., vol. B 111, no. 3, pp.209-219 (1996).
2. Stejskal, EO, Tanner JE. Spin diffusion measurements: spin echoes in the presence of a time-dependent field gradient. J. Chem. Phys. 42:288-292 (1965).
3. Tuch DS. Q-Ball Imaging. Mag. Res. Med. 52:1358-1372, 2004
4. Le Bihan D. IVIM method measures diffusion and perfusion. Diagn Imaging (San Francisco), 12(6):133-136. June 1990
5. Le Bihan D. Magnetic resonance imaging of perfusion. Magn Res Med. 14(2):283-92; May 1990.
6. Hess CP, Mukherjee P, Han ET, Xu D, Vigneron DB. Q-ball reconstruction of multimodal fiber orientations using the spherical harmonic basis. Magn Res Med, 56: 104-117, 2006.
7. Jansons KM, Alexander DC. Persistent angular structure: new insights from diffusion magnetic resonance imaging data. Inverse Probl 2003; 19: 1031-1046.
8. Anderson AW. Measurement of fiber orientation distributions using high angular resolution diffusion imaging. Magn Res Med 2005; 54: 1194-1206.
9. Özarslan E, Shepherd T, Vemuri BC, Blackband S, Mareci T. Resolution of complex tissue microarchitecture using the diffusion orientation transform (DOT). NeuroImage 2006; 31(3): 1083–1106
10. Tournier JD, Calamante F, Gadian D, Connelly A. Direct estimation of the fiber orientation density function from diffusion-weighted MRI data using spherical deconvolution. NeuroImage, 23:1176–1185, 2004.
11. Alexander DC. Maximum entropy spherical deconvolution for diffusion MRI. In: Proceedings of the 19th International Conference on Information Processing in Medical Imaging (IPMI), Glenwood Springs, CO, USA; 2005.
12. Kaden E, Knösche TR, Anwander A. Parametric spherical deconvolution: Inferring anatomical connectivity using diffusion MR imaging. Neuroimage. 37: 474-488, 2007
13. Leow AD, Zhu S, Zhan L, de Zubicaray GI, Meredith M, Wright M, Toga AW, Thompson PM (2008). The Tensor Distribution Function, Mag Res Med, 18; 61(1):205-214.
14. Jones DK, Horsfield MA, Simmons A. Optimal strategies for measuring diffusion in anisotropic systems by magnetic resonance imaging. Mag Res Med 42(3): 515-525. (1999)